Mission Adaptive Compliant Wing – Design, Fabrication and Flight Test

Sridhar Kota, Russell Osborn, Gregory Ervin, Dragan Maric
FlexSys Inc.
2006 Hogback Rd. ,Suite 7
Ann Arbor, MI, U.S.A
kota@flxsys.com

Peter Flick and Donald Paul
Air Force Research Laboratory
Dayton, OH, U.S.A

ABSTRACT

This paper provides an overview of the design, fabrication and testing of a variable camber trailing edge for a high-altitude, long-endurance aircraft. The key enabling technology for the lightweight, low-power adaptive trailing edge is due to utilization of elasticity in the underlying structure through implementation of compliant mechanisms. The paper describes flight testing of the "Mission Adaptive Compliant Wing" (MACW) adaptive structure trailing edge flap used in conjunction with a natural laminar flow airfoil. The MACW technology provides lightweight, low-power, variable geometry re-shaping of the upper and lower flap surface with no seams or discontinuities. In this particular study, the airfoil flap system is optimized to maximize the laminar boundary layer extent over a broad lift coefficient range for endurance aircraft applications. The wing was flight tested at full-scale dynamic pressure, full-scale Mach, and reduced-scale Reynolds Numbers on the Scaled Composites White Knight aircraft. Data from flight testing revealed laminar flow was maintained over approximately 60% of the airfoil chord for much of the lift range. Drag results are provided based on a dynamic pressure scaling factor to account for White Knight fuselage and wing interference effects. The expanded "laminar bucket" capability allows the endurance aircraft to significantly extend its range (15% or more) by continuously optimizing the wing L/D throughout the mission. Future aerodynamic applications and vehicle performance projections are discussed.

Nomenclature

A	=	aspect ratio
C_P	=	pressure coefficient
C_L	=	lift coefficient
C_M	=	quarter chord moment coefficient
g_2	=	total pressure in airfoil wake region
g_∞	=	ambient total pressure
M_∞	=	Mach number
p_2	=	static pressure in airfoil wake region
p_∞	=	ambient static pressure
q_∞	=	ambient dynamic pressure
α	=	angle of attack
α'	=	reduced angle of attack due to wing aspect ratio
γ	=	specific heat ratio of air = 1.4

1.0 INTRODUCTION

FlexSys Inc, under an SBIR program with Air Force Research Lab's (AFRL) Air Vehicles Directorate, has developed a unique, variable-geometry, trailing edge flap that can re-contour the airfoil upper and lower surface [1]. Since the weight of long endurance aircraft can vary by as much as fifty percent (through fuel burn) over the course of a mission, the ability to minimize drag across a wide operating lift coefficient range provides a significant performance increment for any aircraft that incorporates the compliant flap technology. FlexSys has applied the compliant flap system to a Natural Laminar Flow (NLF) airfoil developed for SensorCraft [2] applications. This airfoil can theoretically achieve up to 65% chord laminar flow on the upper surface and up to 90% chord laminar flow on the lower surface. Because NLF airfoils with long laminar runs have steep pressure gradients in the pressure recovery region, the gentle curvature change provided by a compliant flap can reduce or eliminate flow separation over the flap surface as opposed to a conventional hinged flap which can introduce flow separation at the flap knee. Analyses and flight test results indicate that long laminar runs and low drag can be maintained while the compliant trailing edge flap is significantly deflected.

2.0 MISSION ADAPTIVE COMPLIANT WING TECHNOLOGY

Previous efforts to control airfoil camber, as a function of flight condition, utilized multiple actuators distributed throughout the wing. During the 1980's, the Flight Dynamics Laboratory conducted a flight demonstration program called the Mission Adaptive Wing, in which an F-111 was retrofitted with wings whose camber could be actively varied using hydraulic actuators[3]. Figure 1 illustrates the trailing edge actuation and linkage system to vary the camber of the F-111 trailing edge flap. Using conventional rigid-link mechanisms and fiberglass flex-panels, adaptive wing geometry proved its aerodynamic superiority over conventional leading and trailing-edge flaps. Unfortunately, drawbacks in the mechanical design resulted in weight penalties and overall system complexity, significantly offsetting the aerodynamic benefits and prohibited further development. In early 1995, during Phase I of the DARPA-funded Smart Wing Program, a variable wing camber system was investigated that employed inchworm actuators arranged in a truss manner within the wing ribs. Other efforts investigated the effects of changing the shape of a wing using many small actuators distributed throughout a helicopter rotor or a supersonic wing. The most recent of these concepts suggests deployment of a plethora of "intelligent actuators" distributed throughout the system. These distributed actuation concepts generally employ either piezoelectric, shape memory alloy, or TERFENOL-D actuators. Most of these adaptive airfoil concepts suffer from inadequate displacement (piezo actuators), insufficient bandwidth (shape memory actuators), require excessive power, and/or are complex and heavy.

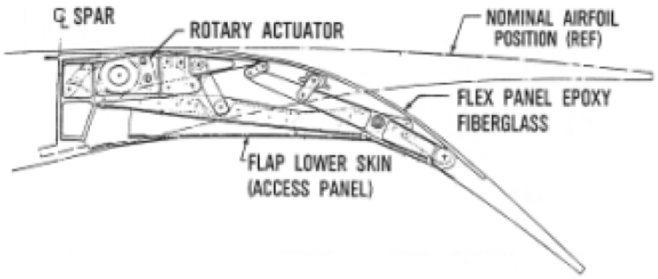

Figure 1: Trailing edge device for the F-111 Mission Adaptive Wing.

Although the shape control of a smart structure involves controlled structural deformation, the *flexibility of the underlying structure* is often not fully exploited. Rather than employing a plethora of actuators to locally

deform an otherwise stiff structure, an alternative approach is to draw energy from a few remotely located actuators and distribute the energy to the structure through some intermediary mechanism. The primary design methodology employed in this effort utilized *distributed compliance rather than distributed actuation* [4, 5]. Compliant Mechanisms (Structures) are structures that are specifically optimized to distribute localized actuation (strain) to effect a net shape change at the control body surface.

In contrast to conventional elastic mechanisms that employ flexible hinges, the Mission Adaptive Compliant Wing (MACW) was developed using sophisticated algorithms to design the topology and shape of an internal structure. This compliant structure deforms as a whole and avoids high-stress concentrations that are indicative of structures designed in which the flexion is concentrated in localized regions. This design paradigm of *distributed* compliance offers additional benefits since the entire adaptive structure is viewed as a compliant mechanism [1] that can move into complex predetermined positions with minimal force and can be locked in place at any desired configuration. While these structures have been described as “flexible,” they are optimized to resist deflection under significant external aerodynamic loading and are just as stiff and strong as a conventional flap [6]. The elimination of discontinuities in the flap surface can provide lower drag and higher control authority than comparable hinged flaps. This is because a compliant flap increases camber under load, generating more lift, and is more effective in roll rates and gust load alleviation per degree of deflection. Furthermore, the elimination of joints and seams make the flap more impervious to icing and fouling from debris.

2.1 Compliant Structures Background

A compliant structure is a monolithic joint-less mechanism that exploits the elasticity of material to produce a desired functionality. These functionalities can include: force or motion transmission, motion guidance, shape morphing, and/or energy storage and release. A compliant *system* consists of actuators and sensors integrated within the compliant structure for transmission [7]. The arrangement of the material within the compliant mechanism is optimized so compliance is *distributed* through small strains to produce large deformations, as shown in Figure 2.

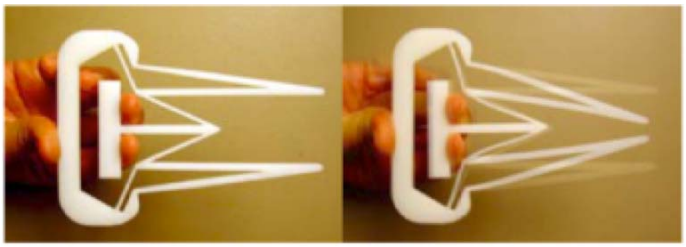

Figure 2: A simple gripper mechanism illustrates the distributed nature of compliance.

Note that the design does not embody any flexural joints, which create stress concentrations and poor fatigue life. In contrast, compliance is distributed to lower maximum stress, thereby significantly improve fatigue life. Just as designs in nature are strong but compliant, so are bio-inspired complaint mechanisms, which enhance "value" in a number of ways:

- Minimize or eliminate assembly requirements;
- Excellent repeatability since there is no backlash;
- No joints means no joint friction, backlash, or need for lubrication;
- Can easily couple with modern actuators, such as piezoelectric, shape-memory alloy, electro-thermal, electrostatic, fluid pressure, and electromagnetic actuators;
- Can create motions not possible with conventional rigid devices;
- Materials friendly: can be built from any highly resilient material, including steel, aluminum, nickel-

titanium alloys, polysilicon, ABS, polypropylene, polymer and metal matrix composites etc.;
- Weight reduction: no need for restoring springs or bulky hinges.
- Fatigue resistant

2.2 Compliant Trailing Edge

While the current research focuses on a trailing edge adaptive structure, FlexSys has developed morphing surfaces for both the leading and trailing edge; and for both fixed wing and rotorcraft applications [8, 9]. Research is targeted at minimizing the force required to morph surfaces while maintaining maximum stiffness to withstand external loading. Design and optimization algorithms account for external (air) loads, actuator force and displacement, morphing shape error, overall system weight, fatigue requirements, buckling forces, and package constraints, while minimizing system complexity. A few design iterations are generally required to resolve conflicting design requirements between aeroelastic behavior and the compliant structure design. Several models have been built and tested to measure aerodynamic and structural performance. A complaint trailing edge flap designed by FlexSys is shown in Figure 3 and demonstrates the flap deflection and twist capability.

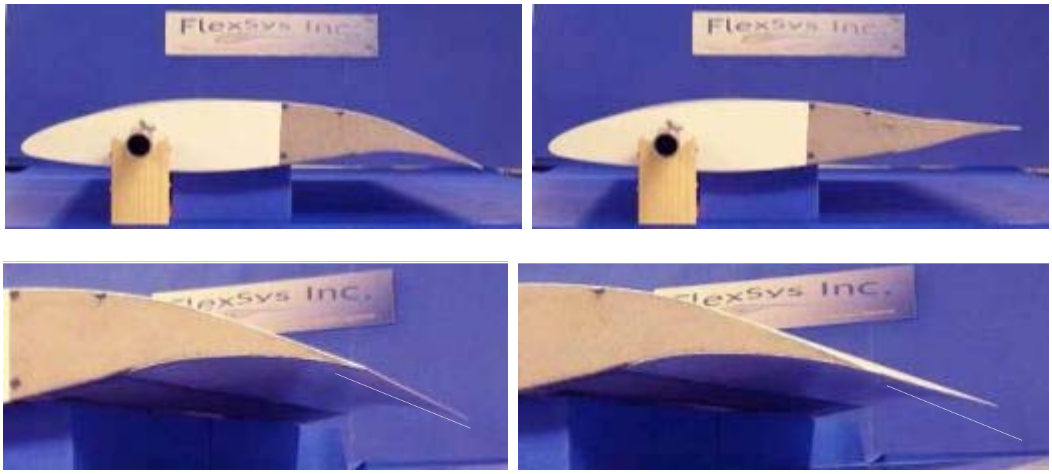

Figure 3: FlexSys Inc.'s Mission Adaptive Compliant Wing trailing edge designed for a high altitude long endurance aircraft undergoing +/- 10^0 flap deflection with a 3^0 twist.

2.3 Potential Benefits – Drag, Weight and Noise reduction

Studies at NASA Dryden show that a mere1% reduction in drag would save the U.S. fleet of wide-body transport aircraft approximately $140 million/year (at a fuel cost of $0.70/gal). There is wide agreement that some sort of "smart wing" could provide optimal wing camber with greatly reduced drag throughout a given cruise envelope. For a medium-range transport aircraft with such a wing, the projected fuel savings is predicted to be 3- 5%, depending on mission distance. After the MAW program, researchers affiliated with Airbus began exploring variable camber wing technology for long and medium-range transport aircraft. Their analysis suggested that a 3-6% reduction in fuel burn might be possible. Aerodynamic results from these studies [3, 10] were quite promising, as indicted in Figure 4. These results [3] appear to offer a substantial mission performance improvement (fuel savings); however, the variable geometry implementation proposed by Airbus required moving, and holding the high lift trailing edge flap during high "q" cruise conditions. The resulting weight penalty in the flap structure/actuation system reduced the estimated performance improvement by one half in the heart of the cruise performance envelope. Airbus and Boeing are now investigating these concepts again as a result of high fuel prices and increased efficiency demand.

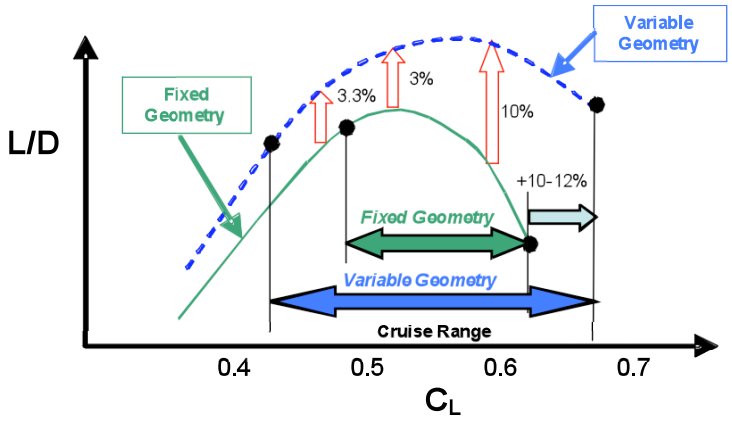

Figure 4: L/D improvement (Airbus A320) with variable geometry trailing edge.

As demonstrated in a Northrop-Grumman study comparison of smart-wing concepts for transonic cruise drag reduction [10], FlexSys has conceptualized an integrated trailing edge that merges the variable camber into the aft element of the high lift flap as shown in Figure 5.

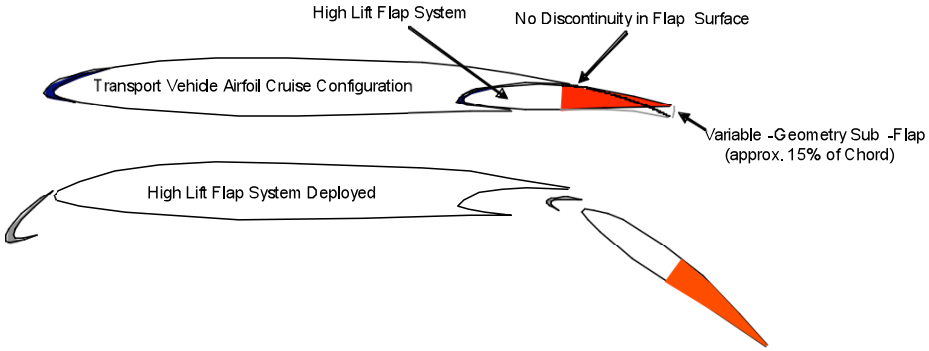

Figure 5: FlexSys high lift flap with cruise variable geometry feature.

The aerodynamic benefits of a smooth, variable camber flap are significant. Comparing equally sized trailing edge flaps, MACW flaps can provide up to a 40% increase in control authority per degree deflection over hinged control surfaces. These gains can be realized with up to 25% lower drag [11]. The boost in aerodynamic performance occurs not only at the aft portion where the trailing edge is located, but over the entire airfoil chord. Forward of the trailing edge, the increased performance is a result of increased circulation and elevated leading edge suction (stagnation point control) created by the variable geometry technology. Figure 6 (a) illustrates aerodynamic analysis of a MACW trailing edge flap performed using XFOIL. Note that laminar flow is maintained for a longer chord percentage for the MACW flap as compared to the conventional (pure rotating) flap. Figure 6 (b) illustrates a direct comparison of the conventional flap L/D performance compared to the MACW flap L/D performance. For instance, at zero degree AOA, the compliant flap achieves nearly a 75% increase in L/D compared to the plain hinged flap.

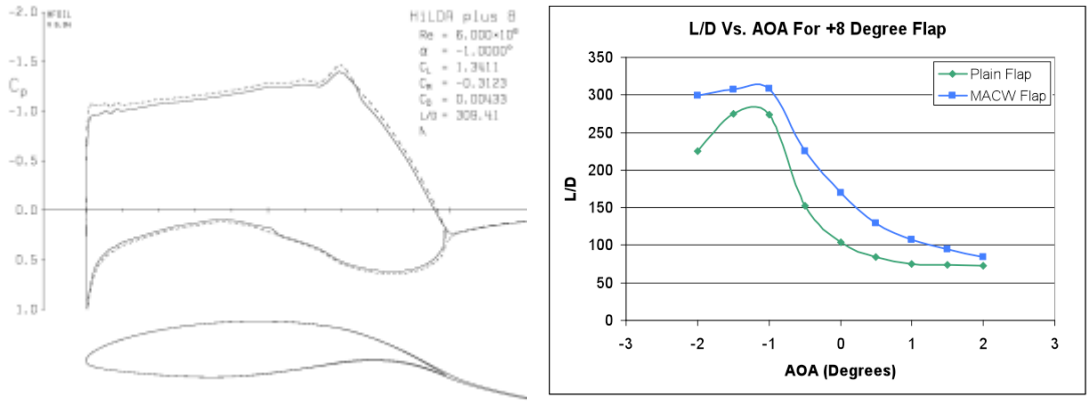

(a) (b)

Figure 6: (a) XFOIL analysis of a plain flap with a +8 degree flap deflection. (b) XFOIL analysis showing L/D comparison of a plain flap and a MACW flap at +8 degree flap deflection.

Finally, MACW technology allows the flap to be positioned with a linearly varying flap deflection along the wingspan. Extensive simulations of the a compliant-flapped wing structure under aerodynamic loading, wing flex, and flap twist, shown in Figure 7, illustrates that these structures can safely withstand a multitude of loads while keeping material strains within their cyclic limits. This differential deflection capability allows a vehicle equipped with MACW flaps to create subtle adjustments to the spanwise lift distribution. This has the benefit of allowing the flap to reshape the wing lift distribution closer to an elliptical distribution, minimizing induced drag and/or reducing the lift levels on outboard sections of the wing in order to minimize the wing root bending moment – thus potentially saving weight.

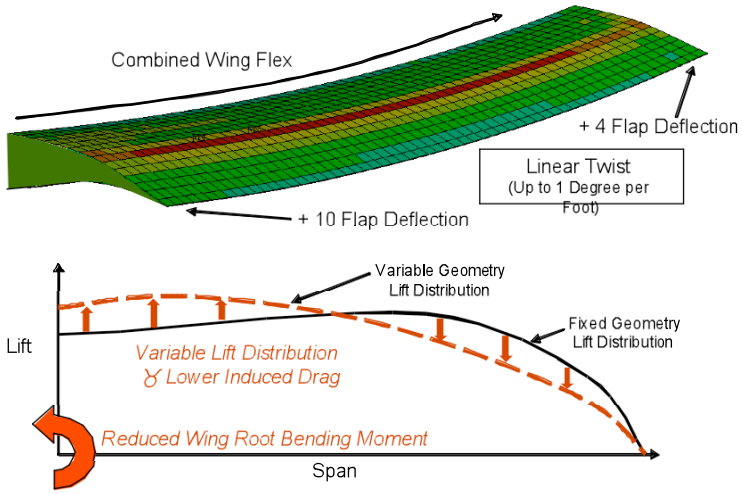

Figure 7: Capability of the MACW control surfaces to produce differential deflection along the span of a wing thereby providing spanwise load tailoring for wing root bending moment control and lift distribution control resulting significant weight savings.

The MACW flight test article was designed to provide a +/- 10º camber change and was fabricated from aircraft grade aluminum. Such a flap can be used as a sub flap to reduce drag during cruise. The shape morphing compliant structure design tools tailored for composite materials demonstrated that large deformations (+40º/-10º flap deflections) could be achieved without exceeding material strength limitations. Therefore, a MACW flap made of composite materials can potentially replace a conventional high lift flap.

Additionally, compliant structures enable development of a seamless transition between the fixed and flapped portions of the wing as shown in Figure 8. The main purpose of this region is to reduce noise associated with the turbulent airflow generated by the discontinuous surfaces at the flap ends when the high lift flaps are deployed for landing. Although the focus of this paper is limited to design and fabrication of an aluminum trailing edge adaptive flap, future applications of the compliant structures technology is likely to be manufactured entirely from composites to obtain large deflections under large loads and include transition regions for noise reduction.

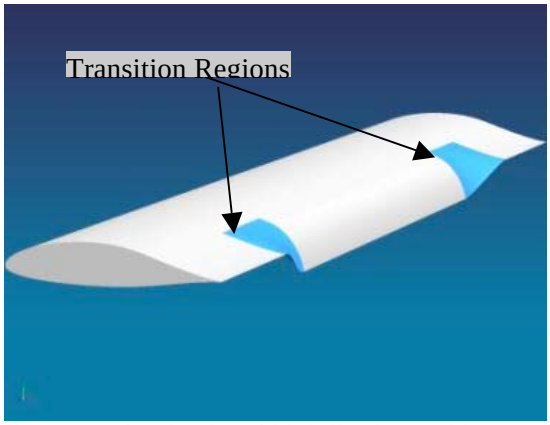

Figure 8: Smooth transition between the fixed and high-lift flaps with composite compliant structures.

In order to produce motion, a MACW flap must elastically strain the underlying flap structure. The required energy to re-shape the structure is minimized during optimization. Even with the additional force required to elastically deform the structure, these flaps work against the aerodynamic loading differently than a hinged flap. Comparing the peak power draw during a high rate movement, MACW flaps can require less force and power than a comparably sized conventional flap. One study comparing a MACW flap to a conventional trailing edge flap during a max G pull-up maneuver showed that the MACW flap required 33% less actuation force and 17% lower peak actuation power. This is because a compliant flap with 33% shorter chord than a conventional flap can provide the same C_L and C_m performance. The moment due to external load is correspondingly smaller for a compliant adaptive flap. Additionally, in a compliant flap the input force from the actuator is applied near the surface (either upper or lower), which provides a longer input moment arm, requiring less input force than a conventional hinged flap.

3.0 HIGH-ALTITUDE LONG ENDURANCE "SENSORCRAFT" APPLICATION

The U.S. Air Force Research Laboratory (AFRL) has identified certain feasible vehicle concepts and aerodynamic technology development requirements for a high-altitude long-endurance intelligence-surveillance-reconnaissance (ISR) concept vehicle known as SensorCraft [2]. SensorCraft is conceived as an unmanned air vehicle system performing command, control, detection, identification, tracking, relay, and targeting functions for long durations at extended ranges. It is the air-breather component of a fully integrated ISR enterprise that incorporates air, space, and ground components.

MACW adaptive structures technology allows the airfoil profile to be tailored to the transitory flight condition (Mach number, wing loading, etc.) over the entire mission. When a natural laminar flow (NLF) airfoil is forced to operate at a higher wing loading (higher lift coefficient) than it is designed for, the leading edge stagnation point moves further aft on the underside of the airfoil and a large suction peak is created as the flow accelerates around the leading edge. This ultimately results in a strong adverse pressure gradient over the

forward part of the upper surface. This adverse pressure gradient forces the boundary layer to transition to turbulent – after which it grows significantly – often creating trailing edge separation. This separation is illustrated in Figure 9 (a) for an airfoil optimized for L/D at C_L=1.0 is forced to operate at C_L=1.2 [12]. As mentioned earlier, a typical SensorCraft platform is expected to burn over half of its weight in fuel on a typical mission. The cruise-climb method of staying near the design lift coefficient is limited by engine specific fuel consumption per Mach and altitude and can be further constrained by sensor requirements. Figure 9 (b) illustrates the potential benefits of using variable geometry compliant structures to produce small, smooth deflections of the trailing edge of a Natural Laminar Flow (NLF) airfoil designed for a representative SensorCraft. Small deflections of the adaptive trailing edge are used to expand the laminar low-drag bucket by controlling the location of the stagnation point and hence the pressure gradient at off-design conditions. This enhanced capability will allow an entire mission to be performed at a reasonably high L/D.

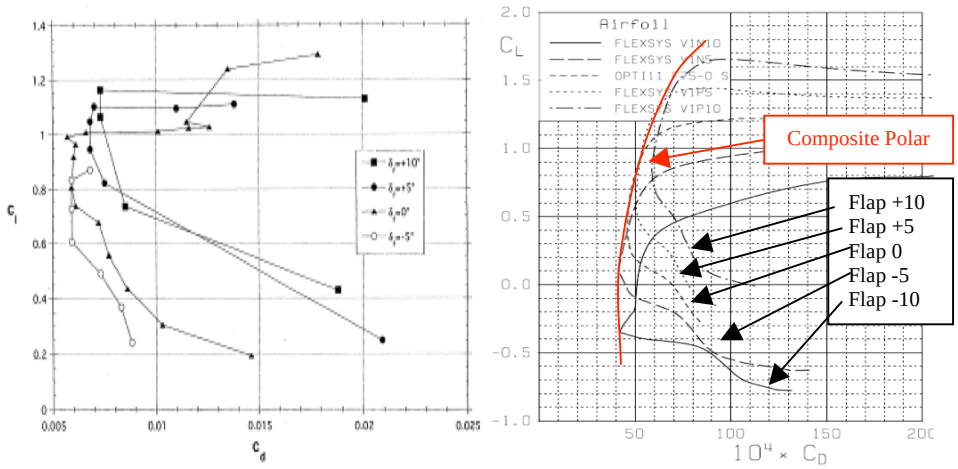

(a) (b)

Figure 9: (a) C_L Vs. C_D experimental data for a modern long endurance airfoil with a conventional trailing edge flap [12]. (b) MSES generated plot showing the composite polar for a MACW flap airfoil.

4.0 FLIGHT TEST MODEL DESCRIPTION

The purpose of the test program was to quantify the aerodynamic and structural performance of a representative MACW prototype system designed for high-altitude, long-endurance aircraft applications in relevant flight environments. The MACW prototype system was flight-tested using the Scaled Composite's White Knight aircraft, an aircraft that is capable of flying at altitude and Mach conditions compatible with long endurance aircraft conditions. The prototype model was designed for an aggressive, 65% chord, laminar boundary layer run on the upper surface that must be maintained over a range of operating lift coefficients using subtle MACW flap deflections. Relevant test conditions were best re-created in the low ambient turbulence, high altitude, flight test environment. Although wind tunnels can simulate conditions compatible with long endurance aircraft conditions, the flight test was preferred due to cost-effectiveness, and the ability to subject the model to the large temperatures fluctuations of Mojave Desert (-60^0 F at 40,000 ft).

4.1 Model Description

The MACW model, shown in Figure 10, has a 50 inches span and 30 inch chord (aspect ratio of 1.67). Elliptical endplates (45" x 24") help bound the flow and reduce three-dimensional effects. The wing is mounted in a cantilever arrangement with all loads channeled through one primary mount (at the bottom of Figure 10). The wing is capable of generating significant force; however, testing was limited to a maximum C_L of 1.2 (roughly 950 lb of lift at flight test condition of 83 psf). During wind tunnel testing at Wright-

Patterson Air Force Base's Subsonic Aerodynamic Research Lab (SARL) facility, the model was subjected to 240 psf loading and was operated at flap rates up to 30^0/sec.

Figure 10: MACW model shown installed in SARL facility.

A structurally optimized variable camber flap, driven by two electrical servo motors embedded within, occupies the last 30% of the model chord. The flap is capable of +/-10 degree change in camber (flap deflection) at rates up to 30 degrees per second (loaded). The variable camber flap-structure is comprised of an upper and lower surface. The upper surface consists of a smooth, continuous surface of an aluminum and polymer composition. The lower surface uses the same composition, but with an additional composite-reinforced panel added extending from 65% to 75% of the model chord. This panel allows the lower surface to expand and contract during flap deflection.

The leading edge of the flight test model is directly machined from 7075-T6 aluminum and holds tolerances as tight as +/- 0.0005" within the first 5% of the model chord. The surface of the model leading edge was ground to a 6 mil surface finish. The model incorporates an angle of attack servo system and a swing arm wake rake servo system. The aluminum leading edge is directly bolted to a heavy-duty turntable bearing that securely fastens the wing to a fixed steel mounting plate. A linear actuator and pivot arrangement, located 15" radially from the turntable bearing center, controls the model angle of attack. A separate servo motor rotates the wake arm to sweep through the airfoil wake region (sweeps across the airfoil height).

With the exception of the compliant trailing edge flap, all structural components maintain safety factors of 8 or greater. The compliant trailing edge flap, due to its need to elastically strain, maintains a static loading safety factor of 2; however, the safety factor with respect to fatigue cyclic loading of this component is considerable (greater than 50). The significant differential between the safety factor and fatigue life is due to the static yield stress governed by the structure geometry and the low prescribed number of morphing cycles the structure sees at that load condition.

The MACW model was mounted from the vertical stub pylon located on the underbelly of the Scaled Composites White Knight. Figure 11 shows the White Knight with the MACW model. During takeoff and landing, the ground clearance from the air data boom of the MACW model to the ground was 20 inches with the tires flat and the landing gear struts fully compressed. The requirement was stipulated by the Air Force Safety Board.

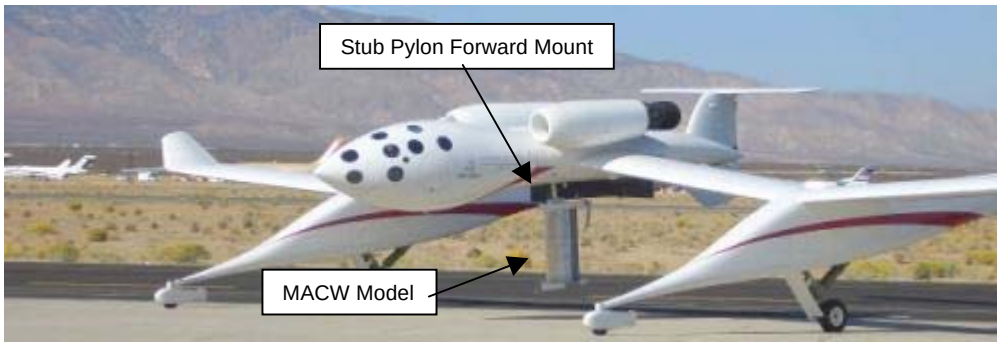

Figure 11: MACW model mounting to Scaled Composites White Knight Aircraft.

4.2 Instrumentation

The following items represent a brief description of all major systems that control, sense, acquire, and store information from the MACW model. Figure 12 shows a schematic of the model data acquisition and control system. A laptop computer serves as the central nervous system to monitor pressures, wake data, hot film data, as well as control angle of attack, the wake rake, and the compliant trailing edge flap servo systems. This computer is programmed using Labview and automates many of the data acquisition processes. Two National Instruments 16-bit, 200 kS/sec USB DAQ boards serve as principle data measurement modules. An RS485 card and cables connects all servo motors to the laptop. Figure 13 shows a screenshot of the data acquisition and control interface.

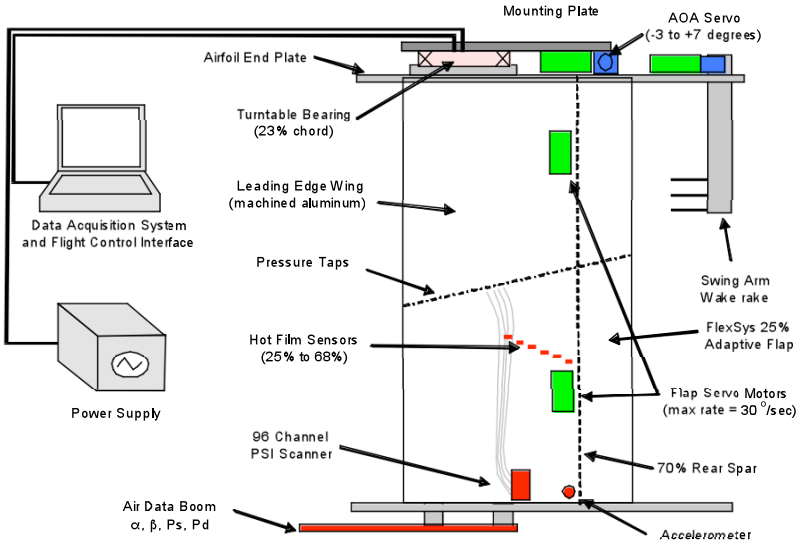

Figure 12: Data Acquisition and Model Control System.

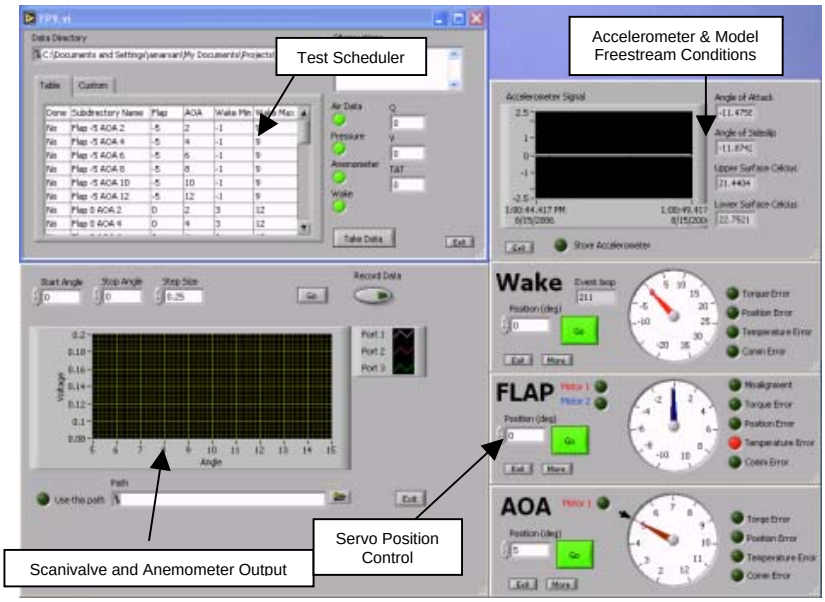

Figure 13: Screenshot of the data acquisition and model control interface.

The model was equipped with a total of 76 0.040" diameter pressure taps – staggered at 15 degrees to prevent upstream laminar flow contamination – which were used to record pressure over the surface of the airfoil. A wake probe with two total and one static pressure probes was used to measure wake pressure profiles at all pertinent test conditions. This unit was mounted to the inboard elliptical end plate. The swing arm probe can traverse +/- 45 degrees to measure the airfoil momentum deficit. Fifteen hot film sensors were arranged to measure the boundary layer transition position. An air data boom was mounted off the outboard elliptical end plate to measure static pressure, total pressure, angle-of-attack and angle-of-sideslip information. An accelerometer was located at the outboard section at 65% chord to monitor model vibrations during flight testing.

5.0 FLIGHT TEST METHOD

Flight testing was conducted at Scaled Composites' facility at the Mojave civilian airport, Mojave, CA. The model was mounted to the underbelly of the White Knight stub pylon's forward fuselage attach point. The aircraft geometry forward of the test section provided a very clean aerodynamic environment with little disturbance of incoming air flow. Two Pratt and Whitney J-85 engines with afterburner powered the White Knight. Thrust capabilities of these engines at high altitude allowed testing at velocities up to Mach 0.55 at 40,000 ft. Test flights were performed over the Isabella MOA airspace. Flight testing was conducted at two primary test points: Mach 0.40 at 25,000 ft and Mach 0.55 at 40,000 ft – with the Mach 0.55 case being the primary case of interest. The Reynolds number at the 25,000 ft test point was 3.3 million; the Reynolds number at the 40,000 ft test point was 2.8 million.

The flight test plan consisted of envelope expansion, natural laminar flow testing and high rate flap demonstration. During envelope expansion, the stability and handling qualities of the White Knight were evaluated at various Mach and altitude test points. At each altitude, the pilot performed a series of maneuvers including stick raps at increasing speed, steady heading sideslips with the wing re-configured to its maximum lift setting and its minimum lift setting, and finally a 2.5 G pull-up maneuver.

After the model handling qualities were cleared at all altitudes and speeds, Natural Laminar Flow testing was

conducted. The natural laminar flow test matrix consisted of 36 test points designed to measure the model lift, drag and pitching moment. Due to the model's finite aspect ratio, the test angle of attack of the model was significantly elevated over the infinite span CFD predictions. This led to rather high model angle of attack positions to push the lift range into the desired C_L = 0.4 to 1.1 test range. Table 1 shows the NLF test matrix for the 40,000 ft test altitude. The data acquisition and control system software allowed the test point scheduler to automatically load the next test point in sequence. This procedure permitted testing to proceed at a rapid pace.

Table 1: AOA and flap deflections for the NLF test matrix showing 36 data points at which lift, drag and pitching moment were measured.

NLF Test Matrix for Test Point A (Mach 0.55 @ 40k ft) Lift and Moment Forces					
AOA (deg) range	**Flap (deg)**	**Estimated C_L range**	**Estimated Lift (lb) range**	**Estimated C_M range**	**Estimated Pitching Moment (ft-lb) range**
2, 4, 6, 8, 10, 12	-5.0	0.11 to 0.92	130 to 714	0.02 to -0.003	37 to -6
2, 4, 6, 8, 10, 12	0	0.36 to 1.16	284 to 902	-0.06 to -0.08	-119 to -148
2, 4, 6, 8, 10, 12	+2.5	0.47 to 1.21	364 to 945	-0.10 to -0.11	-187 to -215
2, 4, 6, 8, 9, 10	+5.0	0.57 to 1.19	448 to 932	-0.13 to -0.15	-254 to -282
2, 4, 6, 7, 8, 9	+7.5	0.68 to 1.19	530 to 931	-0.17 to -0.18	-333 to -354
2, 4, 5, 6, 7, 8	+10.0	0.76 to 1.18	592 to 917	-0.21 to -0.22	-412 to -426

6.0 FLIGHT TEST RESULTS

Flight testing occurred between October and December 2006. A sideslip tolerance of +/- 1 degree (which was AOA for the model) and a velocity tolerance of +/- 2 knots was established by the talented pilots of Scaled Composites. In smooth air, these tolerances were held to tighter levels. Turbulence, however, made holding steady conditions more challenging. The onboard data acquisition systems on the White Knight and the MACW model allowed speed, altitude, and sideslip variability to be monitored. Bug strikes on the leading edge were minimal – only three bug strikes were observed on the leading edge during the entire 27 hours of flight testing.

6.1 Model Surface Pressures

Figures 14 and 15 show the model surface pressures at the Mach 0.55 case at 40,000 ft. In Figure 14, the angle of attack was held constant and the flap deflected to increase the lift generation of the wing. As the flap was deflected, the wing produces more and more lift; however, the pressure gradient on the upper surface over the first 60% of the model chord remained favorable thus keeping the boundary layer laminar.

At roughly 60% model chord, the airfoil geometry contained a subtle bump in the upper surface geometry to trip the boundary layer – as a turbulent boundary layer is more energetic than a laminar boundary layer and can maintain attachment to near the trailing edge surface working against adverse pressure gradients. The steepness of the adverse pressure gradient in this model necessitated a smooth, variable geometry surface to maintain flow attachment – even when flap deflections were small.

In contrast to the case where the AOA was held constant and the flap deflected, Figure 15 displays the C_P curves as the flap was held constant and the AOA increased to vary the lift production. The first 3 angles of

attack from 2 degrees to 6 degrees maintained a favorable pressure gradient on the upper surface. The C_P curve for the angle of attack of 8 degrees and 10 degrees maintained a marginal pressure gradient on the upper surface. The C_P curve for the angle of attack of 12 degrees, required to achieve a lift coefficient of 0.936 had an adverse pressure gradient after the leading edge suction peak – promoting turbulent transition of the boundary layer.

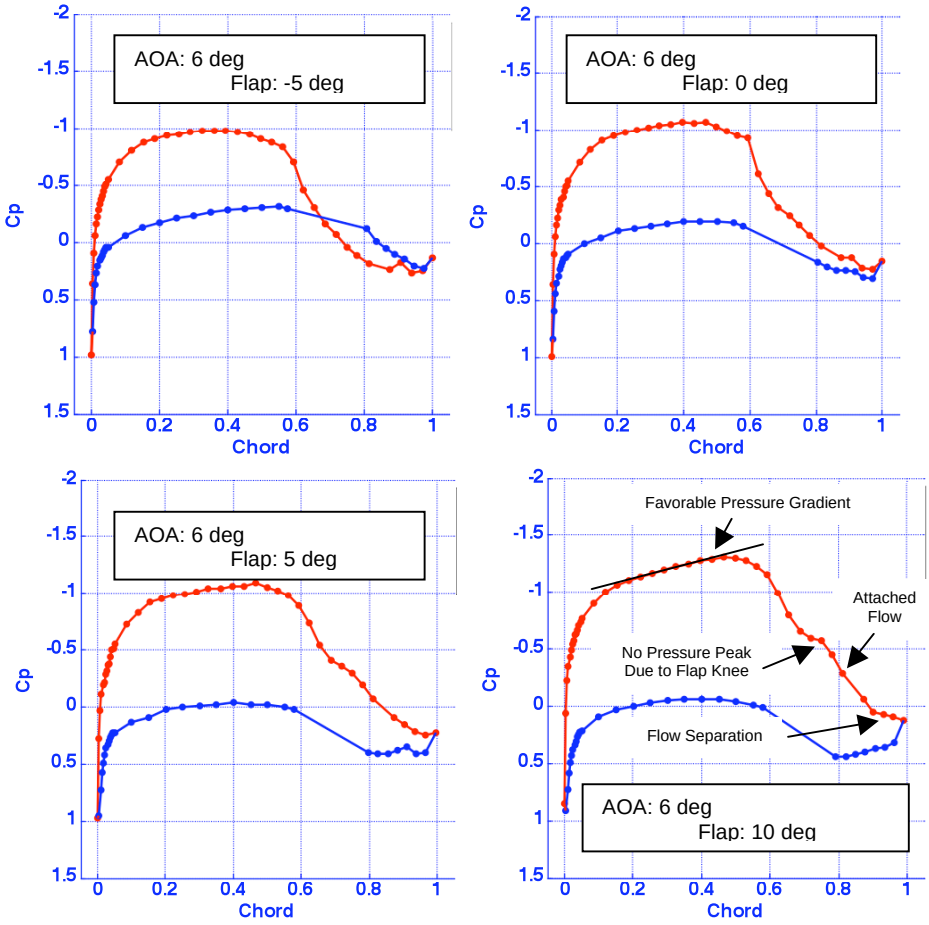

Figure 14: Chord-wise C_P distribution as a function of TE flap deflection for fixed AOA=6^0 showing favorable pressure gradient on the upper surface over the first 60% chord.

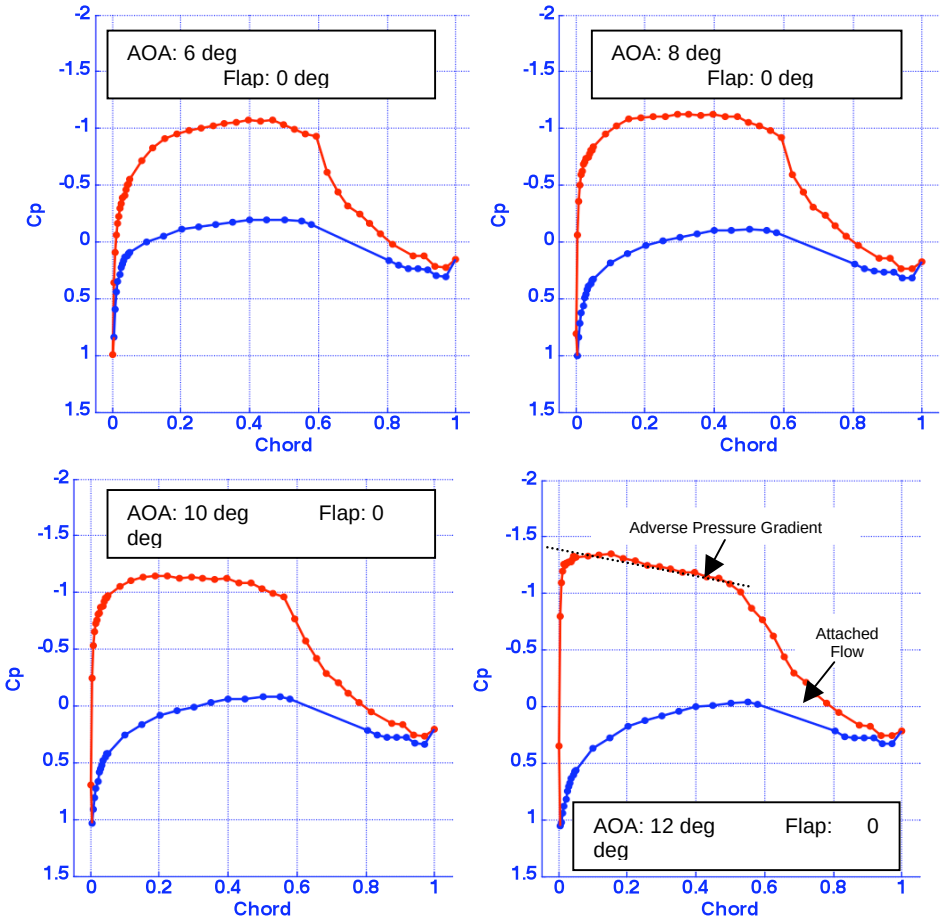

Figure 15: C_P distribution with flap fixed at 0 degrees and AOA varied to change lift levels.

6.2 Model Hot-Film Data

Hot film data was primarily tracked for the model upper surface. Hot films heat a very thin nickel resistive element deposited on a Kapton film to 100 to 150 degrees Celsius. A constant probe temperature is maintained by using carefully derived probe resistance measurements and a measure of the probe's change in resistance per ΔT. Feedback control is performed by the Constant Temperature Anemometer (CTA), which can track up to 8 separate probes simultaneously (each probe has a separate resistance and percent resistivity measurement). A laminar boundary layer (versus a turbulent boundary layer) has a lower rate of convection and a much lower velocity variance. These physical differences show up as changes in the voltage signal output from the CTA (voltage signal is proportional to the probe current).

Hot film data was gathered at 1000 Hz for 8 seconds for each of the 8 films on the upper surface. By comparing a film's voltage amplitude for a "zero White Knight velocity" condition and a "turbulent reference condition" (generated by placing a 0.005" trip strip on the model 5% chord and flying the model at several representative test points), a qualitative determination of whether the boundary layer was laminar or turbulent could be made. Note that a boundary layer does not instantly transition from laminar to turbulent and there are typically intermittency regions where the boundary layer is neither consistently laminar nor turbulent.

Hot film data signals are plotted in Figure 16 for the case of 0 degree flap and 6 degree AOA (CL = 0.589)and

for 10 degree flap deflection and 6 degree AOA (CL = 0.983). Note that the average value of each signal is shifted to avoid overlapping voltage signals. The lower Reynolds number associated with flight testing at 40,000 ft provided a relatively resilient boundary layer and laminar runs could be achieved even with fairly unfavorable pressure gradients.

Figure 16 shows typical cases, with AOA of 6^0 and flap deflections at 0^0 and $+10^0$, with the boundary layer remaining laminar through 53% chord. At 58% chord, the boundary layer was primarily turbulent but with a sharp drop in signal amplitude near the end of the 8 seconds, which signals an intermittency region. At 63% of the chord and beyond, the boundary layer was consistently turbulent. In contrast, the hot-film plot with the flap at $+10^0$and the AOA at 6^0 shows the intermittency region beginning at 58% chord and becoming fully turbulent at 63% chord. Thus even at these higher lift levels, laminar flow is maintained for roughly 10% longer using the compliant flap to generate lift rather than using the model angle of attack. Operation of the model at higher Reynolds numbers would likely make this incremental change in laminar flow chord percentage significantly larger.

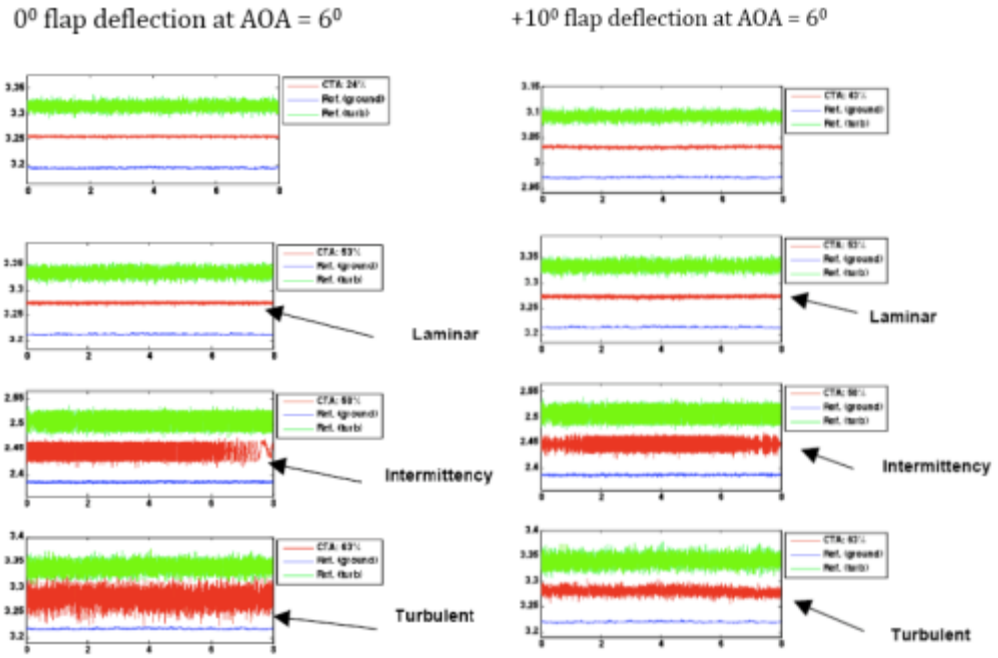

Figure 16: Hot film signals for 0^0 and $+10^0$ flap deflections at 6 degree AOA. Note that the flow transitions to turbulent at about 58% chord.

6.3 Model Experimental Aerodynamics

Data is plotted for the model lift versus angle of attack in Figure 17, pitching moment versus angle of attack in Figure 18, and preliminary model lift to drag behavior in Figure 19. This data was compared to MSES [4] two-dimensional, infinite span results for a wing at the same Mach 0.55, RN = 2.8 million conditions. The largest discrepancy occurred as the lift-curve slope was significantly different than an infinite-span prediction. The reason for these discrepancies was due to the finite aspect ratio of the model. With no endplates, the model maintained an aspect ratio of 1.67; however, the elliptical endplates increased this aspect ratio. Using Equation 1 [6], we compute the model's aspect ratio to be 4.45. Thus, the elliptical endplates improve the wing's aspect ratio from 1.67 to 4.45. Larger endplates would have lessened the aspect ratio effect; however, the drag of the model would have increased to the point where the Mach 0.55 speed was not achievable.

$$\alpha' = \alpha + \frac{C_L}{\pi A} \tag{1}$$

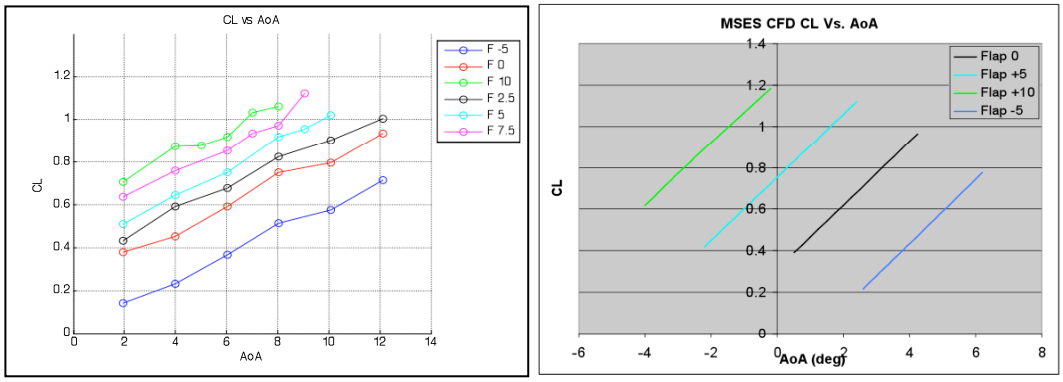

Figure 17: C_L Vs. AOA experimental data for the varying flap deflections compared to MSES 2D CFD predictions.

The aspect ratio also decreases the effectiveness of the flap. For the MSES case, a flap deflection of 5 degrees produces an offset in C_L of 0.088 per degree flap deflection. The experimental data revealed an offset in C_L that measured 0.036 per degree flap deflection. Thus, the finite aspect ratio behavior also affects flap effectiveness.

Moment predictions as compared to MSES 2D CFD are also displayed below. The primary shift in moment production occurred over a much broader angle of attack range. The magnitude of the moment production per flap deflection was largely unaffected by aspect ratio and pitching moment measurements agree relatively well with MSES predictions. Deflecting the flap does, however, produce a significant pitching moment. In practice, this pitching moment would be counteracted by correctly trimming the aircraft.

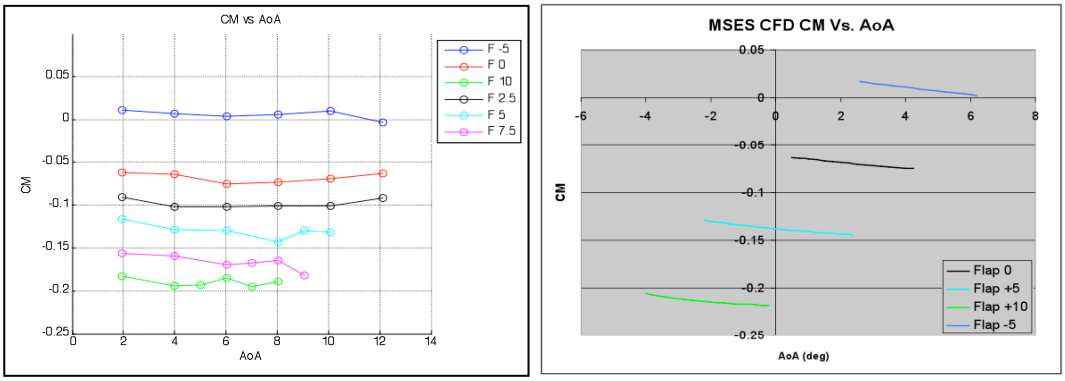

Figure 18: C_M vs. AOA experimental data for the varying flap deflections compared to MSES 2D CFD predictions.

Drag measurements during flight testing were accomplished by sweeping pitot probes (total and static pressure probes) behind the model to survey the momentum deficit. The rotating arm wake rake was favored over a rake fixed to the trailing edge flap due to the ability of the wake to "curl" as a function of model flap deflection and angle of attack. The goal of creating a C_L-C_D plot was to compute an equivalent two-dimensional lift and drag measurement from the MACW test results. This allowed validation of the airfoil

design procedure and the flap performance relative to the MSES CFD tool. Drag polars for the experimental and CFD results are also displayed in Figure 19 for the lift coefficient ranges explored during testing.

Drag levels are calculated using Jones' form of the drag equation, which accounts for the non-zero static pressure field behind the model. The drag equation [13] is shown below:

$$c_D = 2\int_{-\infty}^{+\infty}\sqrt{\frac{g_2 - p_2}{q_\infty}}\left(1 - \sqrt{\frac{g_2 - p_\infty}{q_\infty}}\right)d\left(\frac{y}{l}\right) \qquad (2).$$

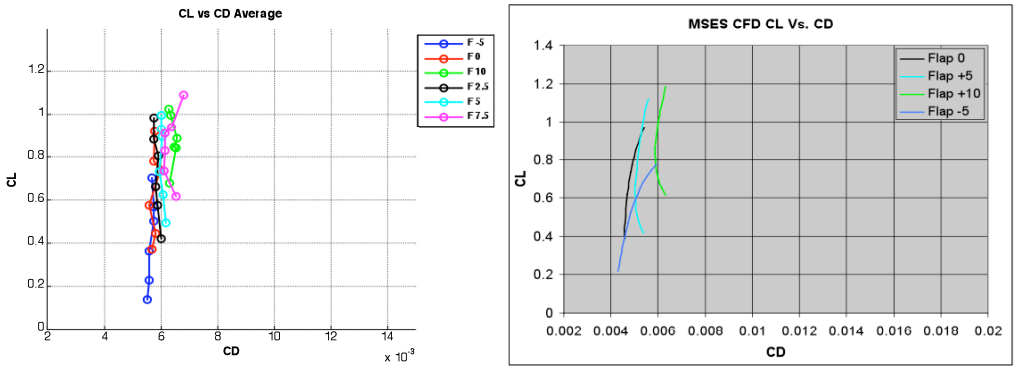

Figure 19: Experimental C_L Vs. C_D for varying flap deflections compared to MSES 2D CFD predictions.

These final drag results, corrected for aircraft flow field, compare favorably with the MSES projections. This opens the door for aggressive laminar flow airfoil designs at elevated Reynolds and Mach numbers for a variety of applications.

6.4 High Rate Flap Testing

Because the MACW technology is primarily limited by the speed of the internal actuator (brushless DC servomotors in this embodiment), high flap deflection rates are achievable. The conclusion of testing involved a high rate demonstration at flap rates up to 30 degrees per second. These rates are compatible with performing Gust Load Alleviation (GLA) for SensorCraft vehicles to alleviate high moment loading (and high stresses) in the wing box. This GLA concept can allow for considerable weight to be pulled from the aircraft wing, allowing further gains in range and endurance. Figure 20 depicts the MACW at 25,000 ft Mach 0.4 moving at a maximum velocity of 30 degrees per second. The success of the high rate capability of the MACW model showed the great potential of this technology to impact SensorCraft and many other aircraft that can benefit from the variable geometry capability.

Figure 20: View from inboard endplate camera showing trailing edge upper surface moving from -10^0 to +10^0 at a 30^0 per second rate.

7.0 CONCLUSIONS AND RECOMMENDATIONS

The mission adaptive compliant flap can effectively control the upper surface pressure distribution while maintaining a sufficiently large transition radius into the pressure recovery region. This geometry minimizes flow separation and airfoil/wing drag. The aerodynamic data (lift, moment, and preliminary drag) measured during the flight test program agree reasonably well with the predicted levels determined computationally using MSES code [14]. The flight test measurements on the wing upper surface confirmed extensive runs of laminar flow (up to 60% chord) even at high operating lift conditions. At the higher Mach flight test point, M = 0.55, 40k ft., the test airfoil lift and moment levels matched the predicted level over the entire airfoil operating lift range.

The MACW flight validation experiment successfully demonstrated that an adaptive compliant trailing edge flap can be successfully designed, manufactured, and operated in an atmospheric environment compatible with long endurance military aircraft mission requirements. And, while it is difficult to determine the exact impact MACW technology might have on specific endurance aircraft without first knowing the configuration, prior Air Force sponsored studies [2] have shown that constant altitude endurance flight may be required to carry fuel loads of 45% to 55% of the aircraft gross weight. The ability to operate at minimum drag over large lift ranges is essential for fuel efficiency and mission success. Examining aerodynamic improvements alone, MACW technology has the potential for increasing the endurance of these air vehicles 15% or more. If gust load alleviation is taken into account or the ability of the flap to twist along the span to further lower wing root bending moment, more dramatic weight savings are suitably envisioned.

Mission adaptive compliant wing technology has been brought to a technology readiness level that will support its application on the next generation high-altitude long-endurance aircraft. As demonstrated during the flight test program, the overall mission performance benefit of a carefully integrated variable camber trailing edge can be substantial. During flight testing, the MACW model was demonstrated at full scale dynamic pressure, Mach, and reduced scale Reynolds numbers. The flap was successfully operated in a high altitude, low temperature environment and did not encounter any operational restrictions or limitations. A final validation of MACW design/fabrication technology to consider might be replacing a trailing edge surface on a flying endurance aircraft with a compliant flap/control. A program of this type would demonstrate fully the aircraft structural integration aspects as well as highlight the lightweight and low power actuation benefits of MACW.

The compliant structure, variable geometry addition to the aft flap element can provide camber control needed to produce performance levels similar to those presented in Figure 19. For example, a medium range transonic transport incorporating the flap system shown is projected to save over 100 gallons of jet fuel on a cross country flight (compliant flap cruise L/D improved 3.3%). Depending on aircraft fuel utilization, a savings of 64,000 gal/yr per aircraft is anticipated.

A flight validation program to verify variable geometry cruise control performance enhancement on a transonic transport aircraft configuration would be beneficial to both future military and commercial aircraft development programs.

8.0 ACKNOWLEDGMENTS

FlexSys Inc. is grateful for the support of Air Force Research Lab RBSA in funding this work. Their continued support has allowed significant and rapid maturation of the MACW technology. FlexSys would also like to thank Dr. Harold Youngren, AeroCraft Consulting for his contribution to the program and to Lockheed Martin for their technical support and input to the model design. Finally FlexSys would like to thank Scaled Composites for their time and talent in helping make the flight test a success and a thoroughly enjoyable experience.

9.0 REFERENCES

1) Kota, S., Hetrick, J., Osborn, R., Paul, D., Pendleton, E., Flick, P. and Tilmann, C., “Design and Application of Compliant Mechanisms for Morphing Aircraft Structures,” Paper 5054-03, *SPIE Smart Struc. and Mat Conf, on Ind. and Comml Appl of Smart Struc Techs*, San Diego CA, March 2003.
2) Tilmann C.P., Flick P.M., Martin C.A., Love, M. H., “High Altitude Long Endurance Technologies for SensorCraft”, *RTO AVT Symposium on “Novel Vehicle Concepts and Emerging Vehicle Technologies”*, Brussels, Belgium, 7-10 April 2003. Published as RTO-MP-104.
3) Greff, E., “The Development and Design Integration of a Variable Camber Wing for Long/Medium Range Aircraft”, *Aeronautical Journal*, November 1990.
4) S. Kota, J.A. Hetrick, R.F. Osborn, “Adaptive Structures: Moving into Mainstream, Aerospace America, September 2006, pp16-18.
5) Lu K-J, S. Kota, Design of Compliant Mechanisms for Morphing Structural Shapes, Journal of Intelligent Materials, Systems, and Structures. Vol. 14, No. 6 page 379-391. 2003.
6) I. H., and von Doenhoff, A. E., *Theory of Wing Sections*, Dover, New York, 1959.
7) Trease and S. Kota, "Design of adaptive and controllable compliant systems with embedded actuators and sensors," *ASME Transactions, Journal of Mechanical Design, MD-7-1387*
8) S. Kota, System for Varying A Surface Contour, U.S. Patent No. 5,971,328, 6, 491, 262
9) S. Kota, J.A Hetrick, Adaptive Compliant Wing and Rotor Systems, US 7,384,016 B1
10) Austin, F., Siclari, M. J., Van Nostrand, W., Kottamasu, V. and Volpe, G., “Comparison of Smart-Wing Concepts for Transonic Cruise Drag Reduction”, *SPIE Smart Structures and Materials Conference*, San Diego, CA, 4-6 March 1997.
11) D.L. Carter, R.F. Osborn, J.A Hetrick, S. Kota, The Quest for Efficient Transonic Cruise, 7th AIAA Aviation Technology, Integration and Operations Conference (ATIO), Sep. 2007, Belfast, Northern Ireland, AIAA 2007-7812.
12) Reed, S.A., “High Altitude Long Endurance Airfoil Performance Validation”, WL-TR-96-3091, Flight Dynamics Directorate, Wright Laboratory, Wright-Patterson AFB, OH, January 1996.
13) Schlichting, H. and Gersten, K., *Boundary Layer Theory*, Eighth Edition, Springer, Berlin, 2000.
14) Giles, M. B., and Drela, M., “Two-Dimensional Transonic Aerodynamic Design Method,” *AIAA Journal*, Vol. 25, No. 9, 1987, pp. 1199-1206.